ACS OMEGA

Open Access

http://pubs.acs.org/journal/acsodf

Article

Discovery of Novel and Selective Schiff Base Inhibitors as a Key for Drug Synthesis, Molecular Docking, and Pharmacological Evaluation

Imran Khan, Wajid Rehman,* Liaqat Rasheed, Fazal Rahim, Rafaqat Hussain, Shoaib Khan, Ashwag S. Alanazi, Mohamed Hefnawy, and Magda H. Abdellattif

Cite This: *ACS Omega* 2024, 9, 31148−31158

Read Online

ACCESS | Metrics & More | Article Recommendations | Supporting Information

ABSTRACT: Diabetes mellitus (DM) is a chronic disorder and still a challenge throughout the world, and therefore the search for safe and effective inhibitors for α-amylase and α-glucosidase is increasing day by day. In this work, we try to carry out the synthesis, modification, and computer-aided results of and biological research on thiadiazole-based Schiff base derivatives and evaluate their *in vitro* α-amylase and α-glucosidase inhibitory potential (**1**−**15**). In the current series, all of the synthesized analogues were shown to have potential inhibitory effects on targeted enzymes. The IC_{50} values for α-amylase values ranged from 20.10 ± 0.40 to 0.80 ± 0.05 μM, compared with the standard drug acarbose having an IC_{50} value of 10.30 ± 0.20 μM, while for α-glucosidase, the IC_{50} values ranged from 20.10 ± 0.50 to 1.20 ± 0.10 μM, compared to acarbose with an IC_{50} value of 9.80 ± 0.20 μM. For better understanding, a SAR investigation was undertaken. In this series, nine scaffolds (**1**, **2**, **3**, **6**, **9**, **10**, **11**, **13**, and **15**) were more active than the reference drug and the docking parameter RMSD values for α-glucosidase and α-amylase were 1.766, 2.7746, 1.6025, 2.2112, 3.5860, 2.3360, 1.6178, 2.0254, and 2.0797 and 2.6020, 1.9509, 3.1642, 1.7547, 2.2130, 1.4221, and 1.1087, respectively. The toxicity of the selected analogues was calculated by using the OSIRIS tool, and the TPSA values were found to be lower than 140 to represent the drug-like properties; those from Molinspiration were studied as well. The following properties were studied and found to have better biological properties. The remaining analogues (**4**, **5**, **7**, **8**, **12**, and **14**) were also identified as potential inhibitors of both enzymes, but they were less active than the reference due to the substituents attached to the aromatic parts. The structures of synthesized compounds were confirmed through different spectroscopic analyses.

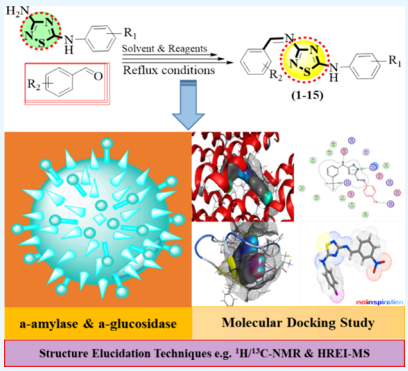

HIGHLIGHTS

- Synthesis of 1,2,4-thiadiazole bearing Schiff base derivatives
- Structure elucidation through different spectroscopic techniques
- *In vitro* evaluation of the synthesized analogues
- Molecular docking and pharmacokinetics analysis

1. INTRODUCTION

Hyperglycemia is a symptom of the chronic metabolic and degenerative disease known as diabetes mellitus (DM). The disease's alarming increase in global incidence over the past few decades has made it a prominent public health issue in the 21st century.[1,2] One of the most common types of DM is noninsulin-dependent diabetes, commonly known to be type 2 diabetes (T2DM), which happens due to insulin resistance. Four hundred twenty-two million people worldwide were estimated to have diabetes as of 2014, up from 108 million in 1980 in the WHO report.[3,4] Furthermore, DM currently ranks as the seventh leading disease in mortality rate worldwide.[5,6] Individuals diagnosed with diabetes may incur various issues as a result of blood vessel impairment and harm to multiple body organs, such as the heart, nerves, kidneys, and eyes.[7−13] The most chemotherapeutic strategy used for managing DM is to regulate postprandial blood glucose levels by blocking the primary enzymes that are responsible for carbohydrate hydrolysis such as α-glucosidase and α-amylase enzymes.[14−16] Both enzymes are essential for the decomposition of disaccharides and sugars, as well as the assimilation of glucose. In addition, the enzymes have the ability to break down polysaccharides into glucose and maltose; through this process, the body glucose level and the negative impact of the disease increase.[17,18] Therefore, it is thought that inhibiting α-glucosidase and α-amylase is a useful tactic in the management of T2DM. Acarbose, voglibose, and miglitol are α-glucosidase and α-amylase inhibitors that have received clinical approval.[19,20] However, these α-glucosidase and α-amylase inhibitors

Received: May 14, 2024
Revised: June 15, 2024
Accepted: June 27, 2024
Published: July 3, 2024

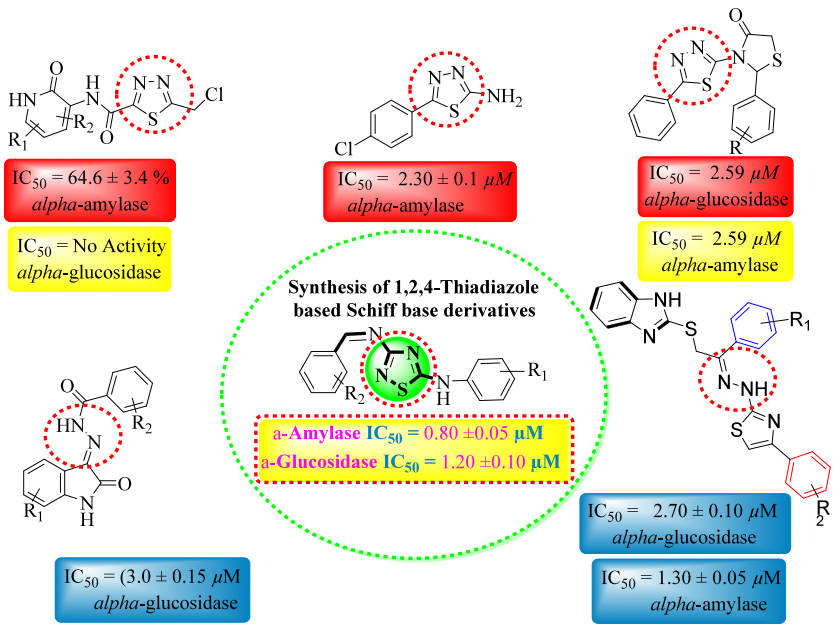

Figure 1. Rationalization of this work.

have been linked to side effects like diarrhea, gastrointestinal problems, and abdominal pain[21−23] and therefore development of novel antidiabetic drugs with increased efficacy and fewer side effects for the treatment of T2DM is required. In the area of medicinal chemistry, 1,2,4-thiadiazoles and Schiff base[24−26] are considered to be the most prominent subgroup of bioactive organic compounds with five-membered ring compounds[27] and display a remarkable range of biological activities, including those for cyclooxygenase inhibition,[28] human leukemia,[29] antibacterial activity,[30,31] ulcerative activity,[32] antihypertensive activity,[33] cathepsin b inhibition,[34] anticonvulsant activity,[35] antidiabetic activity,[36] and allosteric modulators.[37]

DM is one of the most critical and prevalent diseases in this age. However, different routes were adapted to find out the beneficial inhibitors.[38] Due to the diverse range of biological activities that these fused heterocyclic compounds possessed, we were inspired to design and synthesize a new class of heterocyclic compounds like 1,2,4-thiadiazole,[8,39,40] bearing a Schiff base[41,42] in their structure (Figure 1). Different (*E*)-3-((2,4-dichlorobenzylidene)amino)-*N*-(3-(trifluoromethyl)-phenyl)-1,2,4-thiadiazol-5-amine base derivatives were synthesized in this work.

2. RESULTS AND DISCUSSION

2.1. Chemistry. The first step involves the addition of guanidine salt solution (a) to isothiocyanate solution (b) in tetrahydrofuran, with the presence of Et_3N. The resulting mixture was then stirred under reflux for 8 h, resulting in the formation of (c) a substrate. After heating the mixture at a temperature of 80 °C until the reaction was finished, the solvent was removed by evaporating it under reduced pressure. The resultant substrate (c) was then dissolved again in 1,4-dioxane, and iodine and potassium carbonate were added in a specified amount. The resultant residue reflux conditions to the formation of the oxidative N−S bond were fully achieved (the progress of the conversion was analyzed through TLC (thin-layer chromatography), refluxing for the period of 14 h). Once the residue was cooled to a temperature of 25 °C, it was

Scheme 1. Synthesis of Thiadiazole-Based Schiff Base Derivatives

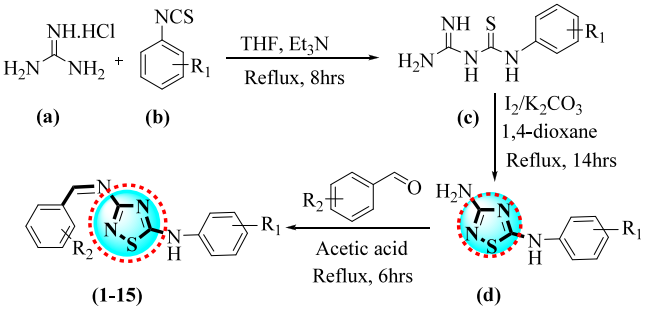

reacted with a 5% solution of sodium thiosulfate and the remaining mixture was then extracted using ethyl acetate, leading to the synthesis of 1,2,4-thiadiazole base (d) as an intermediate. In the last step, the 1,2,4-thiadiazole-base intermediate (d) underwent further reaction with various substituted benzaldehydes in the presence of acetic acid as solvent, resulting in the production of Schiff base derivatives based on 1,2,4-thiadiazole (**1−15**) (Scheme 1).

2.2. Biological Analysis (1−15). *2.2.1. Inhibition Profile of In Vitro α-Amylase and α-Glucosidase.* The inhibition profile of all synthesized analogues bearing 1,2,4-thiadiazole containing a Schiff base moiety was assessed. The SAR (structure−activity relationship) confirmed that newly synthesized thiadiazole-based Schiff base scaffolds demonstrated a remarkable profile toward the selected enzymes, in comparison to standard. Furthermore, SAR studies have suggested that different structural features, including 1,2,4-thiadiazole, Schiff base (C═N), and rings "A" and "B", play a key role in the selected enzymes. Any changes in potency refer to different substitution patterns on both rings.

2.2.2. SAR for Selected Enzymes and Their Inhibition Profile. On the basis of the substitution pattern of both rings, limited SAR studies were discussed for each category, since it was revealed from SAR results that persistent and main structural features such as thiadiazole, the Schiff base of the

https://doi.org/10.1021/acsomega.4c04599
ACS Omega 2024, 9, 31148−31158

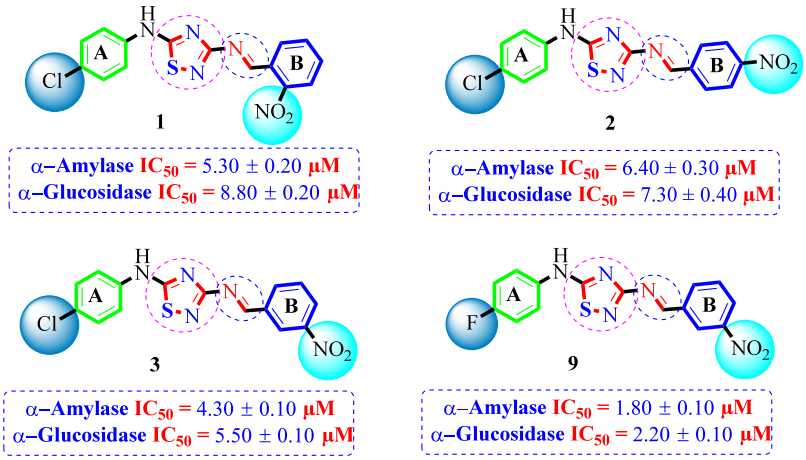

Figure 2. SAR study of compounds **1**, **2**, **3**, and **9**.

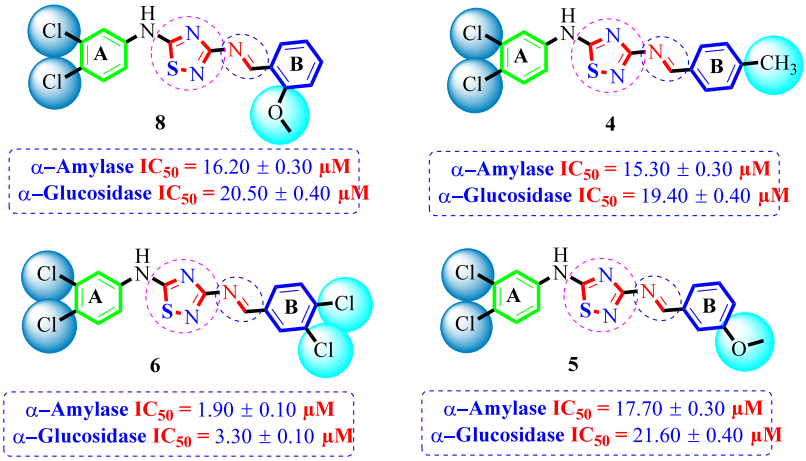

Figure 3. SAR study of compounds **4**, **5**, **6**, and **8**.

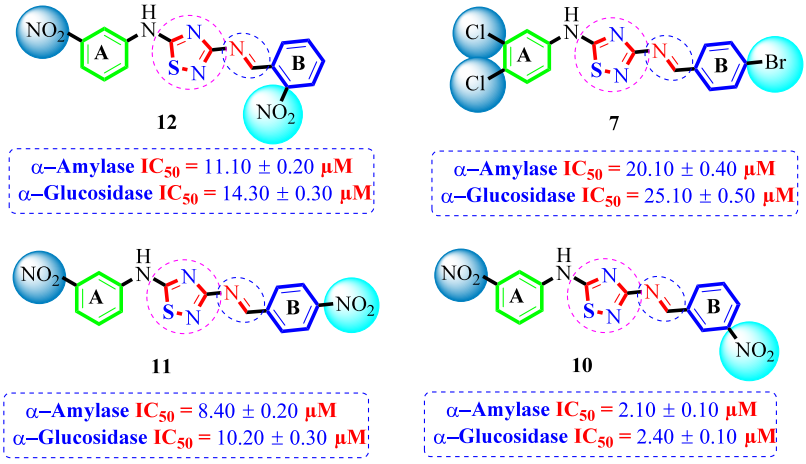

Figure 4. SAR study of compounds **7**, **10**, **11**, and **12**.

aryl part "A" and aryl part "B" moieties, play a key role in inhibiting both targeted enzymes. However, variation around the aryl parts "A" and "B" led to different inhibitory potentials against both enzymes. Compounds **1**−**3** and **9** with a chloro (−Cl) or fluoro (−F) group at the 4-position of the N-aryl portion "A" and a nitro ($-NO_2$) group at various positions of the other aryl component "B" have been found to have remarkable inhibitory activity against both enzymes. Out of all the tested compounds, scaffold **9** showed prominent efficacy against α-amylase and α-glucosidase. These analogues have a −F moiety attached to the aryl part "A" at its 4-position, while the other aryl part "B" carries a moiety $-NO_2$ at its 3-position. These two groups have the ability to effectively engage toward the active part of enzymes, resulting in increased activity. The profile of compound **9** toward enzyme activity decreased when the group attached at the fourth position of ring "A" was

https://doi.org/10.1021/acsomega.4c04599
ACS Omega 2024, 9, 31148−31158

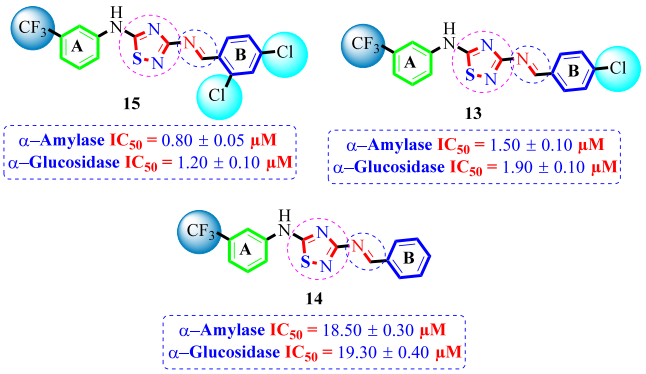

Figure 5. SAR study of compounds **13**, **14**, and **15**.

changed from the −F moiety to the −Cl moiety, similar to analogue **3**. The superior inhibitory profile of compound **9** may be attributed with respect to the strong e-withdrawing nature of −F compared with the −Cl group. Furthermore, scaffold **2**, which is similar to compounds **1** and **3**, exhibits lower potency compared to its structurally different counterparts **1** and **3**. Scaffold **2** contains a $-NO_2$ present at the second position of the aryl part "A" while −Cl is present in the fourth position of the same aryl part. Similarly, compound **3**) as a $-NO_2$ in the third position of ring "B" and a −Cl present in the fourth in the same ring "A". The scaffolds labeled as 1, 2, and 3 have the

Table 2. Thiadiazole Derivatives Representing the Docking Scores and Energy of α-Glucosidase PDB = 3WY1

Cpd	S	Rmsd@refine
1	−5.264	1.766
2	−6.5837	2.7746
3	−6.1562	1.6025
6	−6.0803	2.2112
9	−6.0796	3.5860
10	−6.2323	2.3360
11	−6.2469	1.6178
13	−5.7815	2.0254

Table 1. Inhibitory Potentials of Synthesized Analogues (1−15)

No.	A-ring	B-ring	*alpha*-amylase IC_{50} ± SEM [μM]	*alpha*-glucosidase IC_{50} ± SEM [μM]
1	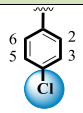		5.30 ± 0.20	8.80 ± 0.20
2	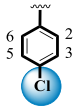	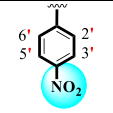	6.40 ± 0.30	7.30 ± 0.40
3	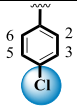		4.30 ± 0.10	5.50 ± 0.10
4	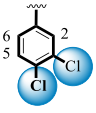	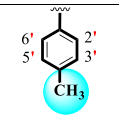	15.30 ± 0.30	19.40 ± 0.40
5	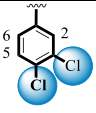	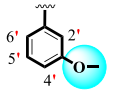	17.70 ± 0.30	21.60 ± 0.40
6	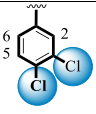	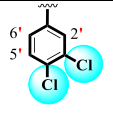	1.90 ± 0.10	3.30 ± 0.10
7	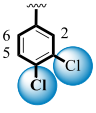	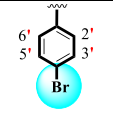	20.10 ± 0.40	25.10 ± 0.50
8	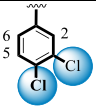		16.20 ± 0.30	20.50 ± 0.40
9	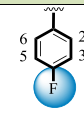		1.80 ± 0.10	2.20 ± 0.10
10	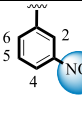		2.10 ± 0.10	2.40 ± 0.10
11	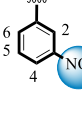		8.40 ± 0.20	10.20 ± 0.30
12	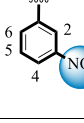		11.10 ± 0.20	14.30 ± 0.30
13	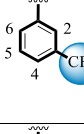	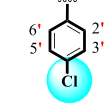	1.50 ± 0.10	1.90 ± 0.10
14	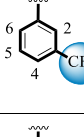	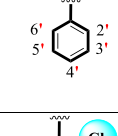	18.50 ± 0.30	19.30 ± 0.40
15	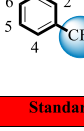	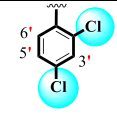	0.80 ± 0.05	1.20 ± 0.10
Standard Acarbose			10 .30 ± 0.20 μM	9.80 ± 0.20 μM

https://doi.org/10.1021/acsomega.4c04599
ACS Omega 2024, 9, 31148−31158

Table 3. Interacting Residues of Thiadiazole Derivatives with α-Glucosidase PDB = 3WY1

Cpd	ligand interaction	receptor	interactions	distance (Å)	E (kcal/mol)
1	O 33	NH1 ARG 124 (C)	H_acceptor	2.93	−2.0
	O 34	NH2 ARG 124 (C)	H_acceptor	2.83	−1.4
	6-ring	6-ring PHE 40 (A)	pi_pi	3.96	−0.0
2	N 2	NH2 ARG 124 (C)	H_acceptor	2.80	−6.4
	6-ring	CG1 VAL 117 (B)	pi_H	4.78	−0.5
3	S 4	O THR 33 (C)	H_donor	3.83	−0.7
	N 6	OE1 GLU 36 (C)	H_donor	2.74	−3.3
6	CL 29	OE2 GLU 43 (B)	H_donor	3.50	−0.6
	CL 30	O THR 33 (C)	H_donor	3.16	−1.0
	N 3	NH1 ARG 124 (A)	H_acceptor	3.12	−2.3
	N 17	NH2 ARG 124 (C)	H_acceptor	3.07	−1.9
	CL 31	N ARG 124 (C)	H_acceptor	3.29	−0.5
	C 18	6-ring PHE 40 (C)	H_pi	4.10	−0.9
	6-ring	CE1 PHE 40 (C)	pi_H	3.53	−0.5
9	S 4	OG1 THR 120 (B)	H_donor	4.28	−0.7
	O 33	NZ LYS 114 (C)	H_acceptor	3.04	−1.2
10	N 2	NH2 ARG 124 (B)	H_acceptor	3.00	−1.7
	5-ring	NH2 ARG 124 (A)	pi_cation	3.53	−0.5
	6-ring	CG2 ILE 121 (C)	pi_H	3.81	−0.7
	6-ring	6-ring PHE 40 (B)	pi_pi	3.69	−0.0
11	S 4	OE1 GLU 36 (A)	H_donor	4.45	−0.8
	N 6	OE1 GLU 36 (B)	H_donor	2.90	−4.4
13	N 6	OE1 GLU 36 (C)	H_donor	2.71	−3.7
	CL 31	NE ARG 127 (C)	H_acceptor	3.46	−0.5
	F 35	NH2 ARG 124 (B)	H_acceptor	2.83	−0.9
	5-ring	NH1 ARG 124 (C)	pi_cation	3.52	−0.8

Table 4. Docking Score Energies of Thiadiazole Analogues with α-Amylase PDB = 4BFH

Cpd	S	Rmsd@refine
1	−5.5608	2.0797
2	−5.4159	2.6020
3	−6.0256	1.9509
6	−5.7133	3.1642
9	−5.8136	1.7547
10	−6.0409	2.2130
11	−5.6153	1.4221
13	−5.5869	1.1087

same structure in terms of the groups attached, such as $-NO_2$ and −Cl groups. However, they differ from each other based on the $-NO_2$ group around the aryl part "B". This indicates that the inhibitory potentials were remarkably influenced by altering the groups from one position to another position of both aryl parts' rings (Figure 2).

Scaffold **6**, which contains two −Cl groups around both rings "A" and "B" present in the same position, demonstrated a potency that was nine times higher than the typical acarbose as a standard drug. The two −Cl groups present in the aromatic rings removed a prominent amount of electronic cloud on both rings, resulting in them becoming electron-deficient species. The activity of scaffold **6** was reduced by a factor of 16 times by removing one −Cl group from the fourth position of aryl group "B" and replacing the other −Cl group from the third position of the same aryl group "B" with a methoxy ($-OCH_3$) group, as seen in scaffold **5**. The difference in potency observed in each of these scaffolds can be attributed to their distinct behavior and the varying number of attached groups. This indicates that both nature and substituent number play a key function in the activity. However, scaffold **8**, which is structurally identical to scaffold **5**, possesses a somewhat better activity than its counterpart **5** but still found as less potent than the standard acarbose drug. Moreover, scaffold **4** displays less potency when compared to analogue **6**. This was due to greater numbers of −Cl moieties present at the third and fourth positions in the ring "B" scaffold (**6**), while compound (**4**) holds only $-CH_3$ present in the fourth position of ring "B" instead the di-Cl groups (Figure 3).

Compound **7** is different from analogue **4** due to the nature of the substituents attached on the rings. Analogue **7** contains a $-CH_3$ present in the fourth position of ring "B", while compound **4** also contains the −Br group similar to the fourth position of ring "B" and scaffold **4** exhibited lower inhibitory potentials compared to the scaffold due to the larger size of the −Br moiety on the fourth position of the aryl component "B". Those groups having a larger size caused steric hindrance, resulting in reduced enzymatic inhibition. In addition, a scaffold **10** that contains $-NO_2$ groups at the third position of both aryl components "A" and "B" was identified as a powerful inhibitor of targeted enzymes. However, the inhibition profile of **10** decreased when the $-NO_2$ group of the aryl component "B" was moved from the third position to the fourth position, as observed in scaffold **11**. The decrease in inhibitory potentials of analogue **10** was further seen by changing the $-NO_2$ group to the second position of the aryl component "B" in scaffold **12**. The scaffolds **10**, **11**, and **12** have a single $-NO_2$ group that is permanently attached to the third position of the aryl part "A". The other aryl component "B" carries a $-NO_2$ moiety at different positions such as second, third, and fourth positions, showing that variation of the $-NO_2$ moiety around aryl part "B" results in different inhibitory potentials. The variation seen in these scaffolds was caused by the differing placement of the $-NO_2$ group on the ring "B" shown in Figure 4.

A scaffold (**15**) with a trifluoro methyl present at the third position of ring "A" and dichloro moieties at the second and fourth positions of ring "B" has been known as an active competitor against both enzymes from all of the synthesized compounds. This scaffold **15** showed many-fold better potency than the standard acarbose drug. The better potency shown by scaffold **15** having more −Cl moieties and an attached trifluoromethyl moiety, which was the withdrawal of electronic

https://doi.org/10.1021/acsomega.4c04599
ACS Omega 2024, 9, 31148−31158

Table 5. Interaction of the Active Residue of Thiadiazole Derivatives with α-Amylase PDB = 4BFH

Cpd	ligand interaction	receptor	interactions	distance (Å)	E (kcal/mol)
1	N 6	O ILE 28 (A)	H_donor	2.84	−1.5
	O 33	N SER 9 (A)	H_acceptor	3.02	−1.2
	O 34	OG SER 9 (A)	H_acceptor	2.70	−1.9
	5-ring	CB CYS 14 (A)	pi_H	4.42	−0.9
2	N 2	N CYS 14 (A)	H_acceptor	2.89	−2.4
	5-ring	CB CYS 29 (A)	pi_H	3.70	−0.6
3	N 6	O TYR 18 (A)	H_donor	2.83	−1.1
	O 33	CA CYS 1 (A)	H_acceptor	3.04	−0.5
	6-ring	N THR 21 (A)	pi_H	4.18	−1.2
6	S 4	OG1 THR 21 (A)	H_donor	3.20	−0.6
	N 6	O ALA 30 (A)	H_donor	2.79	−5.7
	6-ring	CB CYS 1 (A)	pi_H	4.47	−0.6
9	N 6	O TYR 18 (A)	H_donor	2.95	−3.5
	N 2	N CYS 14 (A)	H_acceptor	2.88	−4.2
10	N 6	O GLU 6 (A)	H_donor	2.83	−1.7
	O 35	N HIS 19 (A)	H_acceptor	2.87	−3.7
	6-ring	CB LEU 12 (A)	pi_H	4.41	−0.5
	6-ring	CD1 LEU 12 (A)	pi_H	3.98	−0.5
	6-ring	CB ALA 30 (A)	pi_H	4.14	−0.5
11	N 6	O GLU 6 (A)	H_donor	2.88	−3.2
	6-ring	CA CYS 29 (A)	pi_H	3.57	−0.6
13	N 6	O GLU 6 (A)	H_donor	2.96	−1.3

clouds from ring components "A" and "B", increases their susceptibility to interact with the active pocket of enzymes, resulting in higher enzymatic inhibition. Moreover, the trifluoromethyl moiety has a tendency to interact well through a halogen bond with the active residue of targeted enzymes. In addition, the activity of compound **15** was dropped down by replacing one −Cl group on the second position of ring "B" with a simple hydrogen atom as in analogue **13**, indicating that addition of the −Cl moiety in greater number around aryl part "B" enhanced the enzymatic potentials. Moreover, a further decrease in inhibitory potentials of both scaffolds **13** and **15** was observed by removing either −Cl group from the fourth position of ring "B" or both −Cl moieties at the second and fourth positions of ring "B" in analogue **14** that bear unsubstituted aryl part "B". This scaffold (**15**) holds the $-CF_3$ group in the third position of aryl part "A" along with unsubstituted aryl part "B" that exhibited 17-fold less potency compared to its counterparts **13** and **15**. It was concluded that addition of one or more substituents of electron-withdrawing (EWD) nature such as −Cl around aryl part "B" enhanced the enzymatic potentials as in the case of scaffolds **13** and **15** (Figure 5 and Table 1).

2.3. In Silico Studies. *2.3.1. Molecular Docking.* Recently, docking has had a remarkable rise in molecular docking simulation toward drug discovery and design. Now, the computational technique[43] has proven to be valuable in providing crucial insights on the binding property toward a novel drug and protein being targeted. Hence, it serves as a reliable approach for forecasting the suppression of a specific protein with remarkably reduced time and expenses.[44] A reliable hypothesis is provided toward the mechanism of discovered medicine, which must be further defined. The docking score energy and RMSD results of docked compounds with PDB: 3WY1 and PDB: 4BFH are represented in 2, 3, and 4. The interacting residues of thiadiazole derivatives with α-glucosidase PDB = 3WY1 and α-amylase PDB = 4BFH are represented in Tables 3 and 5, respectively, while the mode of interaction is represented in Figures 6 and 7.

2.3.2. Pharmacokinetics. The expected toxicity was calculated by using the OSIRIS program for analogues **1**, **2**, **3**, **6**, **9**, **11**, and **13**. The outcomes are shown in Table 6. Based on standard therapeutic treatments, these compounds result in having fewer negative side effects. Furthermore, it was shown that certain analogues possess pharmaco-modulation properties and can act as antibiotics respectively (with DS values of 0.53, 0.42, and 0.5). However, these compounds also show reproductive toxicity and have a topological polar surface area (TPSA) greater than 140. It is worth noting that a TPSA score below 140 A 2 is considered ideal for drug-like molecules.

(6) The pharmacokinetic/Molinspiration characteristics for the derivatives **1**, **2**, **3**, **6**, **9**, **10**, **11**, and **13** were determined using Molinspiration online analysis. Mostly analogues showed remarkable potential as such shown in the above docking results. These derivatives showed drug-like characteristics in relation to enzyme, kinase, and protease inhibitors. The activity score distribution (version 2022.08) is related to the scores of GPCR (ligands), ion channel modulators, kinase inhibitors, and nuclear compounds.

3. CONCLUSIONS

In conclusion, thiadiazole-bearing Schiff base derivatives (**1**−**15**) were synthesized and their biological profile was assessed. In order to understand in a better way, a SAR study was conducted. The synthesized derivatives are known as active analogues among the selected enzymes. Among the series, nine scaffolds including **1**, **2**, **3**, **6**, **9**, **10**, **11**, and **13** emerged as active than the standard and their docking parameter RMSD values for α-glucosidase and α-amylase were 1.766, 2.7746, 1.6025, 2.2112, 3.5860, 2.3360, 1.6178, and 2.0254 and 2.0797, 2.6020, 1.9509, 3.1642, 1.7547, 2.2130, 1.4221, and 1.1087, respectively. The toxicity of the selected analogues was calculated by using the OSIRIS tool, and TPSA values lower than 140 were found to represent drug-like properties; those

https://doi.org/10.1021/acsomega.4c04599
ACS Omega 2024, 9, 31148−31158

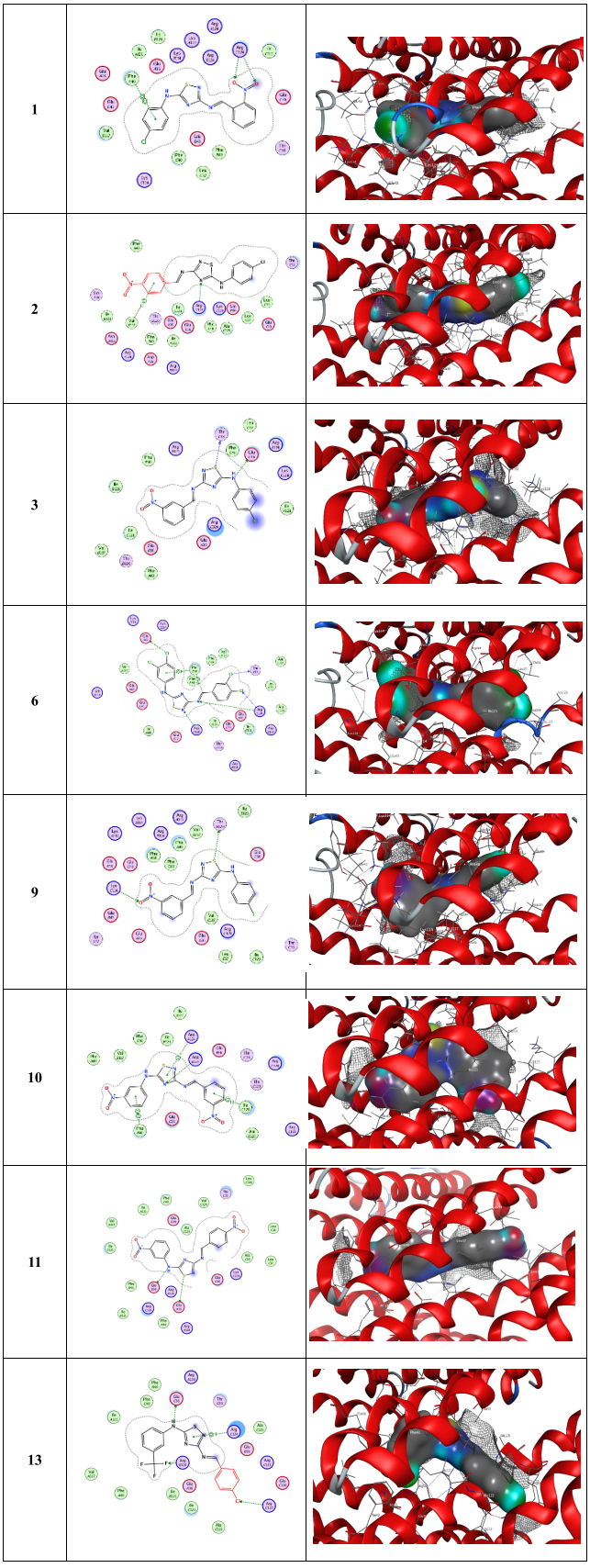

Figure 6. 2D and 3D snaps of interacting residues of thiadiazole derivatives with α-glucosidase PDB = 3WY1.

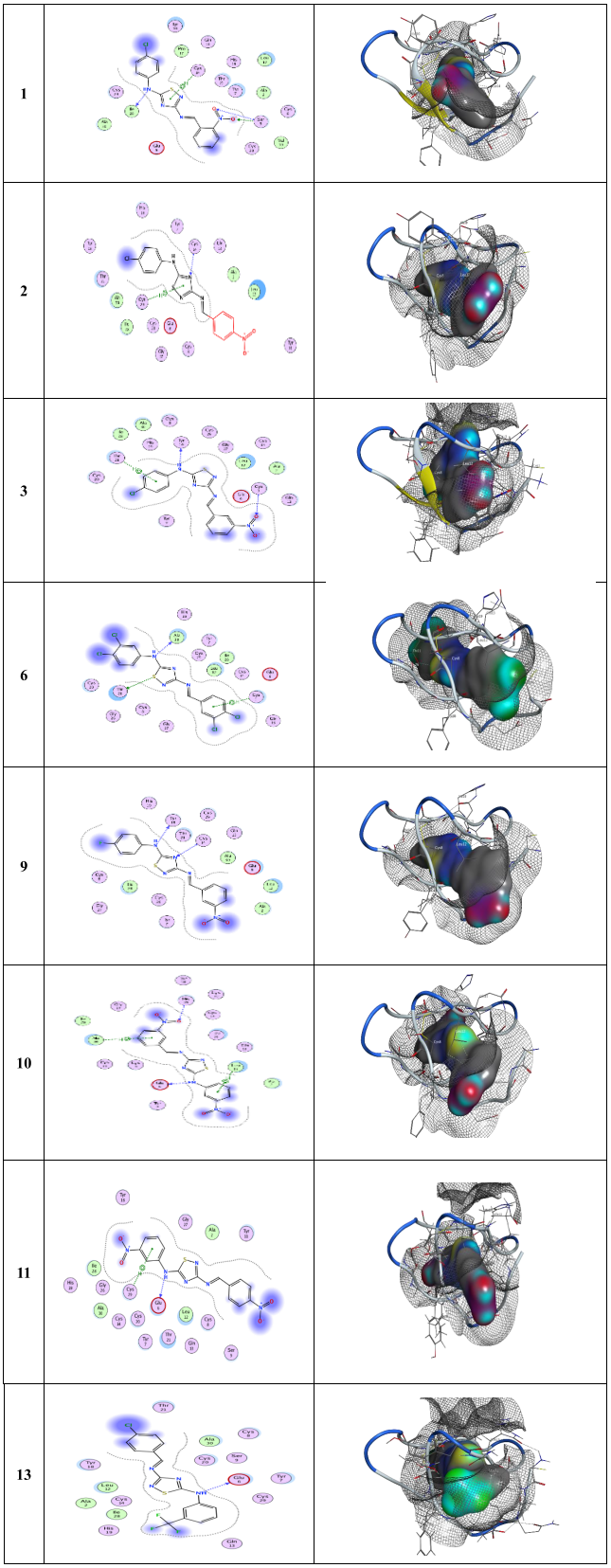

Figure 7. 2D and 3D snaps of interacting residues of thiadiazols' derivatives with alpha-amylase PDB = 4BFH.

from Molinspiration were studied as well. The following properties were studied and found to have better biological properties. NMR and HREI-MS were used for the structural

https://doi.org/10.1021/acsomega.4c04599
ACS Omega 2024, 9, 31148−31158

Table 6. Pharmacokinetics Study of the Selected Analogues

Compound	Bioactivity Scores		Physical Properties	Osiris Properties
1	@GPCR ligand	-0.56	miLogP-4.89 TPSA-96.00 natoms-24 MW-359.80 nON-7 nOHNH-1 nviolations-0 nrotb-5	
	@Ion channel modulator	0.56		
	@Kinase inhibitor	-0.34		
	@Nuclear receptor ligand	-0.67		
	@Protease inhibitor	-0.71	Volume-281.79	Toxicity Risks mutagenic tumorigenic irritant reproductive effective cLogP 4.17 Solubility -4.86 Molweight 359.0 TPSA 124.2 Druglikeness -4.78 Drug-Score 0.3
	@Enzyme inhibitor	-0.28		
2	@GPCR ligand	-0.52	miLogP-4.94 TPSA-96.00 Natoms-24 MW-359.80 nON-7 nOHNH-1 nviolations-0 nrotb-5 Volume-281.79	Toxicity Risks mutagenic tumorigenic irritant reproductive effective cLogP 4.17 Solubility -4.86 Molweight 359.0 TPSA 124.2 Druglikeness -7.84 Drug-Score 0.3
	@Ion channel modulator	-0.54		
	@Kinase inhibitor	-0.27		
	Nuclear receptor ligand	-0.72		
	@Protease inhibitor	-0.70		
	@Enzyme inhibitor	-0.20		
3	@GPCR ligand	-0.53	miLogP-4.92 TPSA-96.00 Natoms-24 MW-359.80 nON-7 nOHNH-1 nviolations-0 nrotb-5 Volume-281.79	Toxicity Risks mutagenic tumorigenic irritant reproductive effective cLogP 4.17 Solubility -4.86 Molweight 359.0 TPSA 124.2 Druglikeness -2.79 Drug-Score 0.32
	Ion channel modulator	-0.56		
	@Kinase inhibitor	-0.27		
	@Nuclear receptor ligand	-0.73		
	@Protease inhibitor	-0.70		
	@Enzyme inhibitor	-0.22		
6	@GPCR ligand	-0.35	miLogP 6.87	
	@Ion channel modulator	-0.48	TPSA 50.17 natoms 24 MW 418.14 nON 4 nOHNH 1 nviolations 1 nrotb 4 volume 299.07	Toxicity Risks mutagenic tumorigenic irritant reproductive effective cLogP 6.91 Solubility -6.61 Molweight 416.0 TPSA 78.41 Druglikeness 0.79 Drug-Score 0.24
	@Kinase inhibitor	-0.11		
	@Nuclear receptor ligand	-0.63		
	@Protease inhibitor	-0.59		
	@Enzyme inhibitor	-0.12		

Compound	Bioactivity Scores		Physical Properties	Osiris Properties
9	@GPCR ligand	-0.52	miLogP-4.40 TPSA-96.00 natoms-24 MW-393.23 nON-7 nOHNH-1 nviolations-0 nrotb-5 Volume-273.19	Toxicity Risks mutagenic tumorigenic irritant reproductive effective cLogP 3.67 Solubility -4.44 Molweight 343.0 TPSA 124.2 Druglikeness -4.86 Drug-Score 0.34
	@Ion channel modulator	-0.56		
	@Kinase inhibitor	-0.22		
	@Nuclear receptor ligand	-0.69		
	@Protease inhibitor	-0.69		
	@Enzyme inhibitor	-0.20		
10	@GPCR ligand	-0.50	miLogP-4.17 TPSA-141.82 natoms-26 MW-370.35 nON-10 nOHNH-1 nviolations-0 nrotb-6 Volume-291.59	Toxicity Risks mutagenic tumorigenic irritant reproductive effective cLogP 2.65 Solubility -4.59 Molweight 370.0 TPSA 170.0 Druglikeness -3.73 Drug-Score 0.36
	@Ion channel modulator	-0.53		
	@Kinase inhibitor	-0.21		
	@Nuclear receptor ligand	-0.70		
	@Protease inhibitor	-0.61		
	@Enzyme inhibitor	-0.18		
11	@GPCR ligand	-0.49	miLogP-4.20	
	@Ion channel modulator	-0.52	TPSA-141.82 natoms-26 MW-370.35 nON-10 nOHNH-1 nviolations-0 nrotb-6 Volume-291.59	Toxicity Risks mutagenic tumorigenic irritant reproductive effective cLogP 2.65 Solubility -4.59 Molweight 370.0 TPSA 170.0 Druglikeness -8.75 Drug-Score 0.35
	@Kinase inhibitor	-0.22		
	@Nuclear receptor ligand	-0.70		
	@Protease inhibitor	-0.60		
	@Enzyme inhibitor	-0.17		
13	@GPCR ligand	-0.30	miLogP-5.85 TPSA-50.17 natoms-25 MW-382.80 nON-4 nOHNH-1 nviolations-1 nrotb-5 Volume-289.76	Toxicity Risks mutagenic tumorigenic irritant reproductive effective cLogP 5.94 Solubility -5.18 Molweight 382.0 TPSA 78.41 Druglikeness -3.72 Drug-Score 0.22
	@Ion channel modulator	-0.40		
	@Kinase inhibitor	-0.05		
	@Nuclear receptor ligand	-0.47		
	@Protease inhibitor	-0.50		
	@Enzyme inhibitor	-0.11		

confirmation. In future, cytotoxic study, identification of lead compounds, refining for selectivity as choice of drugs, in vivo study, and introduction of new groups in the parent compounds will be employed to explore further activities.

4. MATERIALS AND METHODS

4.1. Materials. Analytical-grade solvents and reagents were obtained from Sigma-Aldrich and used without distillation further. TLC (precoated silica gel aluminum plates) was used in this experiment. UV−visible (UV) light was used to view TLC chromatograms at lower 254 and higher 366 nm wavelengths. A mass spectrometer was used to record mass spectra using electron impact (EI). 600 and 150 MHz spectrometers (Bruker Advance AM), ^{1}H-/^{13}C-NMR spectra, were used to record the spectra of the synthesized compounds.

4.2. General Procedure for the Synthesis of 1,2,4-Thiadiazole Derivatives (1−15). The synthesis of 1,2,4-thiadiazole-based derivatives was completed in three steps. In the first step, guanidine salt solution (a) was added into the isothiocyanate solution (b) in the presence of tetrahydrofuran (THF) and Et_3N. The resulting mixture was then stirred under reflux for 8 h, resulting in the formation of (c). After heating

https://doi.org/10.1021/acsomega.4c04599
ACS Omega 2024, 9, 31148−31158

the mixture at the temperature of 80 °C until the reaction was finished, the solvent was evaporated under reduced pressure. The substrate (c) was dissolved in 1,4-dioxane, and iodine and potassium carbonate were added in a specified amount. The mixture was stirred under reflux conditions until the formation of the N−S bond. The residue was cooled to a temperature and treated with a 5% solution of sodium thiosulfate, and the remaining mixture was then extracted using ethyl acetate, leading to the (d) intermediate. Furthermore, the last step intermediate (d) underwent further reaction with various substituted benzaldehydes in the presence of acetic acid as solvent, resulting in the production of Schiff base derivatives based on 1,2,4-thiadiazole (**1**−**15**) (Scheme 1).

4.3. Spectral Analysis. The spectral analysis of the synthesized compounds is found in the Supporting Information.

4.4. Assay Protocol for α-Glucosidase Inhibition. Assay protocol was developed according to the literature reported data.[45]

4.5. Assay Protocol for α-Amylase Inhibition. For the inhibition activity against α-amylase, assay protocol was conducted according to a literature's known method.[46]

4.6. Molecular Docking Study Protocol. The thiadizaole used previously in the human pancreatic enzymes such as α-amylase and α-glucosidase[47] was taken (https://www.rcsb.org/) from the Protein Data Bank (PDB) with the PDB ID: 4BFH and PDB ID: 3WY1. The selection of these proteins was based on a trial of various appropriate enzymes for their interactions with the prepared ligands. Initially, the cocrystallized acarbose obtained by using the proteins was subsequently isolated as an independent molecule and used as the control. The software program known as Molecular Operating Environment (MOE) 2019[48,49] was employed here; this software gained remarkable attention for the preparation of compounds into proteins.[50] Subsequently, at pH 7, hydrogen atoms were employed for obtaining the structure while water molecules were removed by applying the QuickPrep option available in the tool bar of MOE. Prior to validating the docking process, the ligands that were cocrystallized were redocked at the active site of proteins while poses of the molecules were compared with the cocrystallized ligands, their root mean square deviation (RMSD) values being less than 3 Å. The docking results show the presence of four to five orientations for each molecule in relation to the targets. The most flattering stance was determined based on the lowest *S* value.[44] The simulated approximation of ΔG (kcal·mol^{-1}) represents the binding properties, whereas the low RMSD value (Å) indicates minimal disruption in the process. Two metrics are suggested for analyzing the (i) stability of the binding and (ii) the resulting complex between the chemical and the target protein.

4.6.1. OSIRIS Calculation. Thomas Sander created the OSIRIS tool, also known as Osiris Property Explorer, to predict several physicochemical characteristics such as molecular weight, clogP, water solubility, and TPSA. Additionally, it can also assess toxicological properties such as mutagenesis effects, tumorigenicity, irritancy, and reproductive toxicity.[51−53]

4.6.2. Molinspiration Calculation. Molinspiration is offered in different areas of computational biology software, which tell us about the manipulation as well as the processing. The provided tools include the conversion of SD files and SMILES like molecule normalization, formation of tautomers, fragmentation of molecules, calculation of various properties necessary for the quantitative structure−activity relationship (QSAR) used for the molecular docking, drug design, and depiction of high-quality molecules and tools for database, which assist in searches for the substrate.[43,51]

■ ASSOCIATED CONTENT

Supporting Information

The Supporting Information is available free of charge at https://pubs.acs.org/doi/10.1021/acsomega.4c04599.

Spectral analysis (PDF)

■ AUTHOR INFORMATION

Corresponding Author

Wajid Rehman − *Department of Chemistry, Hazara University, Mansehra 21120, Pakistan;* orcid.org/0000-0003-0128-0377; Email: sono_waj@yahoo.com

Authors

Imran Khan − *Department of Chemistry, Hazara University, Mansehra 21120, Pakistan*

Liaqat Rasheed − *Henan International Joint Laboratory of Nano-Photoelectric Magnetic Material, School of Material Science and Engineering, Henan University of Technology, Zhengzhou, Henan 450001, China*

Fazal Rahim − *Department of Chemistry, Hazara University, Mansehra 21120, Pakistan*

Rafaqat Hussain − *Department of Chemistry, Hazara University, Mansehra 21120, Pakistan*

Shoaib Khan − *Department of Chemistry, Abbottabad University of Science and Technology (AUST), Abbottabad 22010, Pakistan*

Ashwag S. Alanazi − *Department of Pharmaceutical Sciences, College of Pharmacy, Princess Nourah bint Abdulrahman University, Riyadh 11671, Saudi Arabia*

Mohamed Hefnawy − *Department of Pharmaceutical Chemistry, College of Pharmacy, King Saud University, Riyadh 11451, Saudi Arabia*

Magda H. Abdellattif − *Department of Chemistry, College of Sciences, Taif University, Taif 21944, Saudi Arabia;* orcid.org/0000-0002-8562-4749

Complete contact information is available at: https://pubs.acs.org/10.1021/acsomega.4c04599

Notes

The authors declare no competing financial interest.

■ ACKNOWLEDGMENTS

The authors extend their appreciation to Princess Nourah bint Abdulrahman University researcher supporting project number (PNURSP2024R342), Princess Nourah bint Abdulrahman University, Riyadh, Saudi Arabia, for supporting this work. The authors also extend their appreciation to the Researchers Supporting Project number (RSPD2024R754), King Saud University, Riyadh 11451, Saudi Arabia, for supporting this work.

■ REFERENCES

(1) The Emerging Risk Factors Collaboration. Diabetes mellitus, fasting blood glucose concentration, and risk of vascular disease: a collaborative meta-analysis of 102 prospective studies. *Lancet* **2010**, *375* (9733), 2215−2222.

(2) Rodriguez-Saldana, J. *The diabetes textbook: Clinical principles, patient management and public health issues*; Springer Nature, 2023.
(3) Pradeepa, R.; Mohan, V. Epidemiology of chronic complications of diabetes: A global perspective. In *Chronic Complications of Diabetes Mellitus*; Elsevier, 2024; pp 11−23.
(4) Rahman, T. *A Proposed Method to Identify the Occurrence of Diabetes in Human Body Using Data Analysis*. 2023.
(5) Organization, W. H. *WHO Global report on diabetes*. 2016.
(6) Khan, M. F.; Jamil, B.; Senneville, E. Diabetes and infections. In *BIDE's Diabetes Desk Book*; Elsevier, 2024; pp 527−561.
(7) Saeedi, P.; Petersohn, I.; Salpea, P.; Malanda, B.; Karuranga, S.; Unwin, N.; Colagiuri, S.; Guariguata, L.; Motala, A. A.; Ogurtsova, K.; Shaw, J. E.; Bright, D.; Williams, R. Global and regional diabetes prevalence estimates for 2019 and projections for 2030 and 2045: Results from the International Diabetes Federation Diabetes Atlas. *Diabetes research and clinical practice* **2019**, *157*, No. 107843.
(8) Gummidi, L.; Kerru, N.; Ebenezer, O.; Awolade, P.; Sanni, O.; Islam, M. S.; Singh, P. Multicomponent reaction for the synthesis of new 1, 3, 4-thiadiazole-thiazolidine-4-one molecular hybrids as promising antidiabetic agents through α-glucosidase and α-amylase inhibition. *Bioorganic Chemistry* **2021**, *115*, No. 105210.
(9) Shaw, J. E.; Sicree, R. A.; Zimmet, P. Z. Global estimates of the prevalence of diabetes for 2010 and 2030. *Diabetes research and clinical practice* **2010**, *87* (1), 4−14.
(10) Susan van, D.; Beulens, J. W. J.; Yvonne T. van der, S.; Grobbee, D. E.; Nealb, B. The global burden of diabetes and its complications: an emerging pandemic. *European Journal of Cardiovascular Prevention & Rehabilitation* **2010**, *17* (1_suppl), s3−s8.
(11) Li, Y.; Liu, Y.; Liu, S.; Gao, M.; Wang, W.; Chen, K.; Huang, L.; Liu, Y. Diabetic vascular diseases: molecular mechanisms and therapeutic strategies. *Signal transduction and targeted therapy* **2023**, *8* (1), 152.
(12) Antar, S. A.; Ashour, N. A.; Sharaky, M.; Khattab, M.; Ashour, N. A.; Zaid, R. T.; Roh, E. J.; Elkamhawy, A.; Al-Karmalawy, A. A. Diabetes mellitus: Classification, mediators, and complications; A gate to identify potential targets for the development of new effective treatments. *Biomedicine & Pharmacotherapy* **2023**, *168*, No. 115734.
(13) Nithya, V.; Sangavi, P.; Srinithi, R.; Nachammai, K.; Gowtham Kumar, S.; Prabu, D.; Langeswaran, K. Diabetes and other comorbidities: Microvascular and macrovascular diseases diabetes and cancer. In *Advances in Diabetes Research and Management*; Springer, 2023; pp 21−39.
(14) Oyewusi, H. A.; Wu, Y.-S.; Safi, S. Z.; Wahab, R. A.; Hatta, M. H. M.; Batumalaie, K. Molecular dynamics simulations reveal the inhibitory mechanism of Withanolide A against α-glucosidase and α-amylase. *J. Biomol. Struct. Dyn.* **2023**, *41* (13), 6203−6218.
(15) Durgam, M. K.; Vemuri, P. K.; Bodiga, V. L.; Bodiga, S. Lupenone Isolated from Diospyros melanoxylon Bark Non-competitively Inhibits alpha-amylase Activity. *Biology, Medicine, & Natural Product Chemistry* **2022**, *12* (1), 171−176.
(16) Kashtoh, H.; Baek, K.-H. New insights into the Latest advancement in α-amylase inhibitors of plant origin with anti-diabetic effects. *Plants* **2023**, *12* (16), 2944.
(17) Yi, J.; Li, L.; Yin, Z.; Quan, Y.; Tan, R.; Chen, S.; Lang, J.; Li, J.; Zeng, J.; Li, Y.; Sun, Z.; Zhao, J. Polypeptide from Moschus Suppresses Lipopolysaccharide-Induced Inflammation by Inhibiting NF-κ B-ROS/NLRP3 Pathway. *Chinese Journal of Integrative Medicine* **2023**, *29*, 895−904.
(18) Zuo, W.; Zuo, L.; Geng, X.; Li, Z.; Wang, L. Radical-Polar Crossover Enabled Triple Cleavage of CF2Br2: A Multicomponent Tandem Cyclization to 3-Fluoropyrazoles. *Org. Lett.* **2023**, *25*, 6062−6066.
(19) S.H.N. Moorthy, N.; J. Ramos, M.; A. Fernandes, P. Studies on α-glucosidase inhibitors development: magic molecules for the treatment of carbohydrate mediated diseases. *Mini reviews in medicinal chemistry* **2012**, *12* (8), 713−720.
(20) Zhang, Z.; Zhang, W.; Hou, Z.; Li, P.; Wang, L. Electrophilic Halospirocyclization of N-Benzylacrylamides to Access 4-Halomethyl-2-azaspiro[4.5]decanes. *Journal of Organic Chemistry* **2023**, *88*, 13610−13621.
(21) Chen, L.; Jiang, Z.; Yang, L.; Fang, Y.; Lu, S.; Akakuru, O. U.; Huang, S.; Li, J.; Ma, S.; Wu, A. HPDA/Zn as a CREB Inhibitor for Ultrasound Imaging and Stabilization of Atherosclerosis Plaque. *Chin. J. Chem.* **2023**, *41*, 199−206.
(22) Ali, F.; Khan, K. M.; Salar, U.; Taha, M.; Ismail, N. H.; Wadood, A.; Riaz, M.; Perveen, S. Hydrazinyl arylthiazole based pyridine scaffolds: Synthesis, structural characterization, in vitro α-glucosidase inhibitory activity, and in silico studies. *Eur. J. Med. Chem.* **2017**, *138*, 255−272.
(23) Jiang, Z.; Shi, H.; Tang, X.; Qin, J. Recent advances in droplet microfluidics for single-cell analysis. *TrAC Trends in Analytical Chemistry* **2023**, *159*, No. 116932.
(24) Tskhovrebov, A. G.; Novikov, A. S.; Odintsova, O. V.; Mikhaylov, V. N.; Sorokoumov, V. N.; Serebryanskaya, T. V.; Starova, G. L. Supramolecular polymers derived from the PtII and PdII Schiff base complexes via C (sp2)−H··· Hal hydrogen bonding: Combined experimental and theoretical study. *J. Organomet. Chem.* **2019**, *886*, 71−75.
(25) Sysoeva, A. A.; Novikov, A. S.; Suslonov, V. V.; Bolotin, D. S.; Il'in, M. V. 2, 1, 3-Benzoselenadiazole-containing zinc (II) halide complexes: Chalcogen bonding in the solid state and catalytic activity in the Schiff condensation. *Inorg. Chim. Acta* **2024**, *561*, No. 121867.
(26) Lystsova, E. A.; Novokshonova, A. D.; Khramtsov, P. V.; Novikov, A. S.; Dmitriev, M. V.; Maslivets, A. N.; Khramtsova, E. E. Reaction of Pyrrolobenzothiazines with Schiff Bases and Carbodiimides: Approach to Angular 6/5/5/5-Tetracyclic Spiroheterocycles. *Molecules* **2024**, *29* (9), 2089.
(27) Kumar, D.; Maruthi Kumar, N.; Chang, K. H.; Shah, K. Synthesis and anticancer activity of 5-(3-indolyl)-1, 3, 4-thiadiazoles. *European journal of medicinal chemistry* **2010**, *45* (10), 4664−4668.
(28) Unangst, P. C.; Shrum, G. P.; Connor, D. T.; Dyer, R. D.; Schrier, D. J. Novel 1, 2, 4-oxadiazoles and 1, 2, 4-thiadiazoles as dual 5-lipoxygenase and cyclooxygenase inhibitors. *Journal of medicinal chemistry* **1992**, *35* (20), 3691−3698.
(29) Wang, Q.; Guo, Q.; Niu, W.; Wu, L.; Gong, W.; Yan, S.; Nishinari, K.; Zhao, M. The pH-responsive phase separation of type-A gelatin and dextran characterized with static multiple light scattering (S-MLS). *Food Hydrocolloids* **2022**, *127*, No. 107503.
(30) Harai, R.; Sakamoto, K.; Hisamichi, H.; Nagano, N. Structure-activity relationships of cephalosporins having a (dimethylisoxazolidinio) vinyl moiety at their 3-position. *Journal of Antibiotics* **1996**, *49* (11), 1162−1171.
(31) Zayda, M. G.; Abdel-Rahman, A. A.-H.; El-Essawy, F. A. Synthesis and antibacterial activities of different five-membered heterocyclic rings incorporated with pyridothienopyrimidine. *ACS omega* **2020**, *5* (11), 6163−6168.
(32) Kharimian, K.; Tam, T.; Leung-Toung, R.; Li, W. Thiadiazole compounds useful as inhibitors of hb/kb atpase. *PCT Int. Appl.* WO9951584A1 1999.
(33) Jiang, Z.; Han, X.; Zhao, C.; Wang, S.; Tang, X. Recent Advance in Biological Responsive Nanomaterials for Biosensing and Molecular Imaging Application. *International Journal of Molecular Sciences* **2022**, *23*, 1923.
(34) Liu, K.; Jiang, Z.; Zhao, F.; Wang, W.; Jäkle, F.; Wang, N.; Tang, X.; Yin, X.; Chen, P. Triarylboron-Doped Acenethiophenes as Organic Sonosensitizers for Highly Efficient Sonodynamic Therapy with Low Phototoxicity. *Adv. Mater.* **2022**, *34*, 2206594.
(35) Castro, A.; Castaño, T.; Encinas, A.; Porcal, W.; Gil, C. Advances in the synthesis and recent therapeutic applications of 1, 2, 4-thiadiazole heterocycles. *Bioorganic & medicinal chemistry* **2006**, *14* (5), 1644−1652.
(36) Pragathi, Y. J.; Sreenivasulu, R.; Veronica, D.; Raju, R. R. Design, synthesis, and biological evaluation of 1, 2, 4-thiadiazole-1, 2, 4-triazole derivatives bearing amide functionality as anticancer agents. *Arabian journal for science and engineering* **2021**, *46*, 225−232.
(37) Shen, F.; Long, D.; Yu, T.; Chen, X.; Liao, Y.; Wu, Y.; Lin, X. Vinblastine differs from Taxol as it inhibits the malignant phenotypes

https://doi.org/10.1021/acsomega.4c04599
ACS Omega 2024, 9, 31148−31158

of NSCLC cells by increasing the phosphorylation of Op18/stathmin. *Oncol. Rep.* **2017**, *37*, 2481−2489.
(38) Zhang, J.; Zhong, A.; Huang, G.; Yang, M.; Li, D.; Teng, M.; Han, D. Enhanced efficiency with CDCA co-adsorption for dye-sensitized solar cells based on metallosalophen complexes. *Sol. Energy* **2020**, *209*, 316−324.
(39) Palamarchuk, I. V.; Shulgau, Z. T.; Dautov, A. Y.; Sergazy, S. D.; Kulakov, I. V. Design, synthesis, spectroscopic characterization, computational analysis, and in vitro α-amylase and α-glucosidase evaluation of 3-aminopyridin-2 (1 H)-one based novel monothiooxamides and 1, 3, 4-thiadiazoles. *Organic & Biomolecular Chemistry* **2022**, *20* (45), 8962−8976.
(40) Wang, H.; Shang, Y.; Wang, E.; Xu, X.; Zhang, Q.; Qian, C.; Yang, Z.; Wu, S.; Zhang, T. MST1 mediates neuronal loss and cognitive deficits: A novel therapeutic target for Alzheimer's disease. *Progress in Neurobiology* **2022**, *214*, No. 102280.
(41) Deng, P.; Dong, X.; Wu, Z.; Hou, X.; Mao, L.; Guo, J.; Zhao, W.; Peng, C.; Zhang, Z.; Peng, L. Development of Glycosylation-Modified DPPA-1 Compounds as Innovative PD-1/PD-L1 Blockers: Design, Synthesis, and Biological Evaluation. *Molecules* **2024**, *29*, 1898.
(42) Hussain, R.; Iqbal, S.; Shah, M.; Rehman, W.; Khan, S.; Rasheed, L.; Rahim, F.; Dera, A. A.; Kehili, S.; Elkaeed, E. B.; Awwad, N. S.; Bajaber, M. A.; Alahmdi, M. I.; Alrbyawi, H.; Alsaab, H. O. Synthesis of novel benzimidazole-based thiazole derivatives as multipotent inhibitors of α-amylase and α-glucosidase: in vitro evaluation along with molecular docking study. *Molecules* **2022**, *27* (19), 6457.
(43) Baykov, S. V.; Mikherdov, A. S.; Novikov, A. S.; Geyl, K. K.; Tarasenko, M. V.; Gureev, M. A.; Boyarskiy, V. P. $\pi-\pi$ noncovalent interaction involving 1, 2, 4-and 1, 3, 4-oxadiazole systems: The combined experimental, theoretical, and database study. *Molecules* **2021**, *26* (18), 5672.
(44) Cheng, F.; Li, W.; Zhou, Y.; Shen, J.; Wu, Z.; Liu, G.; Lee, P. W.; Tang, Y. admetSAR: a comprehensive source and free tool for assessment of chemical ADMET properties. *ACS Publications*: **2012**. DOI: 10.1021/ci300367a
(45) Ramírez-Escudero, M.; Gimeno-Pérez, M.; González, B.; Linde, D.; Merdzo, Z.; Fernández-Lobato, M.; Sanz-Aparicio, J. Structural analysis of β-fructofuranosidase from Xanthophyllomyces dendrorhous reveals unique features and the crucial role of N-glycosylation in oligomerization and activity. *J. Biol. Chem.* **2016**, *291* (13), 6843−6857.
(46) Salar, U.; Khan, K. M.; Chigurupati, S.; Taha, M.; Wadood, A.; Vijayabalan, S.; Ghufran, M.; Perveen, S. New hybrid hydrazinyl thiazole substituted chromones: As potential α-amylase inhibitors and radical (DPPH & ABTS) scavengers. *Sci. Rep.* **2017**, *7* (1), 16980.
(47) Wang, X.; Deng, Y.; Zhang, Y.; Zhang, C.; Liu, L.; Liu, Y.; Jiang, J.; Xie, P.; Huang, L. Screening and Evaluation of Novel α-Glucosidase Inhibitory Peptides from Ginkgo Biloba Seed Cake Based on Molecular Docking Combined with Molecular Dynamics Simulation. *J. Agric. Food Chem.* **2023**, *71* (27), 10326−10337.
(48) Gul, S.; Jan, F.; Alam, A.; Shakoor, A.; Khan, A.; AlAsmari, A. F.; Alasmari, F.; Khan, M.; Bo, L. Synthesis, molecular docking and DFT analysis of novel bis-Schiff base derivatives with thiobarbituric acid for α-glucosidase inhibition assessment. *Sci. Rep.* **2024**, *14* (1), 3419.
(49) Shehab, W. S.; Abdellattif, M. H.; Mouneir, S. M. Heterocyclization of polarized system: synthesis, antioxidant and anti-inflammatory 4-(pyridin-3-yl)-6-(thiophen-2-yl) pyrimidine-2-thiol derivatives. *Chemistry Central Journal* **2018**, *12*, 1−8.
(50) Shehab, W. S.; Elsayed, D. A.; Abdel Hamid, A. M.; Assy, M. G.; Mouneir, S. M.; Hamed, E. O.; Mousa, S. M.; El-Bassyouni, G. T. CuO nanoparticles for green synthesis of significant anti-Helicobacter pylori compounds with in silico studies. *Sci. Rep.* **2024**, *14* (1), 1608.
(51) Abdellattif, M. H.; Hamed, E. O.; Elhoseni, N. K. R.; Assy, M. G.; Emwas, A.-H. M.; Jaremko, M.; Celik, I.; Titi, A.; Kumar Yadav, K.; Elgendy, M. S.; Shehab, W. S. Synthesis of novel pyrazolone candidates with studying some biological activities and in-silico studies. *Sci. Rep.* **2023**, *13* (1), 19170.
(52) Adesina, A. F.; Adewuyi, A.; Otuechere, C. A. Exploratory studies on chrysin via antioxidant, antimicrobial, ADMET, PASS and molecular docking evaluations. *Pharmacological Research-Modern Chinese Medicine* **2024**, *11*, No. 100413.
(53) Nunes, I. J.; Dias, R. F.; da Silva, A. F.; Ferreira, W. V.; Cunico, W.; Couto, G. T.; Bianchini, D.; Casagrande, O. d. L., Jr; Saffi, J.; Pinheiro, A. C. Exploring the structure-activity relationship (SAR) of Schiff bases as effective compounds in scavenging free radicals. *J. Mol. Struct.* **2024**, *1315*, No. 138729.

https://doi.org/10.1021/acsomega.4c04599
ACS Omega 2024, 9, 31148−31158